MISR Multi-angle Imaging Spectro-Radiometer

Jet Propulsion Laboratory **Interoffice Memorandum**

MISR SCIENCE DFM #231

October 13, 2000

To: Carol J. Bruegge

From: Nadine C. Lu Chrien

Subject: MISR On-Board Calibrator performance

This memorandum is intended to summarize the studies performed to evaluate the MISR On-Board Calibrator. The radiance measured by the PIN photodiodes using their preflight calibrations did not agree well with the radiances returned by the HQE photodiodes or with the radiance predicted using the bidirectional reflectance factor (BRF) measurements of the calibration panels, solar zenith angle, Earth-Sun distance, and the MISR standardized response weighted exo-atmospheric solar irradiance. The decision was made to re-calibrate the OBC using on-orbit data and using the HQE blue photodiode as the standard.

Included in this document are comparisons of predicted versus measured radiances for all calibration data to date starting with orbit 1076, along with results for both preflight and in-flight calibrations of the OBC. The results indicate a degradation in the NIR HQE photodiode response. This is not unexpected and is likely due to radiation exposure. It does, however, point to a need to recalibrate the OBC prior to each calibration. Also, indicated is a degradation in the green bands of all the PIN photodiodes, an unexpected result for which no explanation currently exists.

The OBC files used in this study and their orbits and dates are listed in Table 1.

Table 1: List of On-Board Calibrator data files used in this work

Filename	Orbit	Date	Pole
MISR_AM1_FM_OBC_CL_P151_O000076_01.hdf	1076	01mar2000	North and South
MISR_AM1_FM_OBC_CL_P050_O001259_01.hdf	1259	13mar2000	North
MISR_AM1_FM_OBC_CL_P231_O001314_01.hdf	1314	17mar2000	North
MISR_AM1_FM_OBC_CL_P230_O001911_01.hdf	1911	27apr2000	North
MISR_AM1_FM_OBC_CL_P013_O001912_01.hdf	1912	27apr2000	South
MISR_AM1_FM_OBC_CL_P136_O002575_01.hdf	2575	12jun2000	North
MISR_AM1_FM_OBC_CL_P063_O002585_01.hdf	2585	12jun2000	South
MISR_AM1_FM_OBC_CL_P001_O003717_01.hdf	3717	29aug2000	North
MISR_AM1_FM_OBC_CL_P065_O003721_01.hdf	3721	29aug2000	South

The predicted radiance viewed by a given photodiode is calculated as follows:

$$L^{\text{std, OBC}}_{\text{predicted}} = \frac{\cos\theta_i \;\; \text{BRF}(\theta_i, \varphi_i; \theta_r^{\text{OBC}}, \varphi_r^{\text{OBC}}) \;\; E_0^{std}}{\pi} \;\; \frac{R_0^2}{R^2} \qquad (1)$$

where,

θ_i, φ_i are the solar zenith and azimuth angles, respectively, measured from the panel normal

$\theta_r^{OBC}, \varphi_r^{OBC}$ are the reflected zenith and azimuth angles, respectively, as viewed by a given OBC photodiode

E_0^{std} is the standardized response weighted exo-atmospheric solar irradiance

R_0 is the geocentric distance between the Sun and Earth at which E_0^{std} was measured (1 AU)

R is the geocentric distance between the Sun and Earth in astronomical units (AU), and is computed based upon the calibration date using equations from Barbara Gaitley's *ephemeris.pro* code.

The radiance measured by a given photodiode is computed as follows:

$$L_{\text{measured}}^{\text{std, OBC}} = \frac{1.2395 i E_0^{std}}{(A\Omega) k} \tag{2}$$

$$= \int_{200nm}^{1200nm} E_{0,\lambda} R_\lambda \lambda d\lambda \tag{3}$$

where,

i is the measured photodiode current in nA

$A\Omega$ is the area*solid angle product or étendue for the OBC photodiode

R_λ is the spectral response function of the OBC photodiode

$E_{0,\lambda}$ is the spectral exo-atmospheric solar irradiance function

k is the photodiode calibration correction factor

In the case of preflight diode calibrations, k= 1. The calibration correction factor is computed based upon the assumption that the Spectralon® calibration panels are spectrally flat, Lambertian targets. This implies that the ratio of one diode current to another should equal the ratio of étendue-response products, $A\Omega$ (equation 4). The calibration correction factors for the nadir viewing diodes are computed using the blue HQE diode and its preflight calibration as the standard, i.e., $k_{HQE,\,blue} = 1$ (equation 5). The D-diodes, PIN-3 and PIN-4, are calibrated to the blue HQE diode using the goniometer, PIN-G, as a transfer standard. The goniometer calibration correction factor is computed using currents when the goniometer position is nadir-viewing. The D-diode bands are then calibrated to the goniometer diode bands as shown in equation 6.

$$\left[\frac{i_2}{(A\Omega)_2 k_2} = \frac{L_2^{\text{std,OBC}}}{E_{0,2}^{std}} = \frac{L_1^{\text{std,OBC}}}{E_{0,1}^{std}} = \frac{i_1}{(A\Omega)_1 k_1}\right] \quad \left(\frac{i_2}{i_1}\right) = \frac{(A\Omega)_2}{(A\Omega)_1}\left(\frac{k_2}{k_1}\right) \tag{4}$$

$$k_{\text{diode, band}} = \frac{i_{\text{diode, band}}}{i_{\text{HQE, blue}}} \div \frac{(A\Omega)_{\text{diode, band}}}{(A\Omega)_{\text{HQE, blue}}} \tag{5}$$

$$k_{\text{D-diode,band}} = \frac{i_{\text{D-diode,band}}}{i_{\text{goni, band @D-angle}}} \div \frac{(A\Omega)_{\text{D-diode,band}}}{(A\Omega)_{\text{goni, band}} k_{\text{goni, band}}} \tag{6}$$

The current ratios are computed using the mean diode currents during the time the goniometer is running. This time frame is identified using the data OK flag of field 12 of the rad_qual table in the OBC HDF files. In SDFM#230, the goniometer on/off times were taken from a PACKSCAN analysis of the Level 0 ENG files. This results in a slight difference (0.0001 for the green, red, and NIR HQE

diodes) in the calibration correction factors listed in this memorandum for Orbit 1259 from those found in SDFM#230.

The calibration correction factors represent the average correction factor computed for Cal-North and Cal-South with the exception of the D-diode factors. For the D-diode factors, the north-south average is applied to the PIN-G for the transfer, but PIN-3 only views the south panel and PIN-4 only views the north panel. The photodiode integrated response functions and AΩ-products are listed in Table 2 and Table 3. The calibration correction factors for each calibration sequence are given in Table 4 through Table 9.

Table 2: diode integrated solar-weighted spectral response, [W m^{-1}]

diode		Band			
position	type	BLUE	GREEN	RED	NIR
+Y	PIN-1	13.0698	14.3526	8.7570	11.4217
-Y	PIN-2	13.0104	14.9508	8.7721	12.1682
Df	PIN-3	15.4890	14.5350	8.6580	11.5130
Da	PIN-4	16.0568	15.5577	10.8097	11.6961
goniometer	PIN-G	12.6824	14.2086	11.1406	10.9881
+Y (B, G), -Y (R, N)	HQE	17.3235	11.6565	12.5182	16.1813

Table 3: diode étendue or AΩ [m^2 sr]

Diode		Band			
position	type	BLUE	GREEN	RED	NIR
+Y	PIN-1	1.4806E-08	1.4829E-08	1.4755E-08	1.4653E-08
-Y	PIN-2	1.4803E-08	1.4813E-08	1.4766E-08	1.4674E-08
Df	PIN-3	1.4786E-08	1.4793E-08	1.4738E-08	1.4623E-08
Da	PIN-4	1.4752E-08	1.4783E-08	1.4786E-08	1.4783E-08
goniometer	PIN-G	1.4796E-08	1.4830E-08	1.4806E-08	1.4779E-08
+Y (B, G), -Y (R, N)	HQE	7.4541E-09	7.4495E-09	7.4719E-09	7.4730E-09

Table 4: diode calibration correction factors computed using Orbit 1076 (Cal-North and Cal-South), HQE blue as standard

Diode		Band			
position	type	BLUE	GREEN	RED	NIR
+Y	PIN-1	0.8907	0.9056	0.9191	0.8991
-Y	PIN-2	0.8962	0.8600	0.9025	0.8593
Df	PIN-3	0.8915	0.8809	0.9144	0.8939
Da	PIN-4	0.8526	0.8315	0.8956	0.8567
goniometer	PIN-G	0.9252	0.9038	0.9093	0.8897
+Y (B, G), -Y (R, N)	HQE	1.0000	1.0405	0.9575	1.0955

Table 5: diode calibration correction factors
computed using Orbits 1259 (Cal-North) and 1912 (Cal-South), HQE blue as standard

Diode		Band			
position	type	BLUE	GREEN	RED	NIR
+Y	PIN-1	0.8929	0.8869	0.9178	0.8942
-Y	PIN-2	0.8989	0.8469	0.8996	0.8541
Df	PIN-3	0.8834	0.8549	0.9035	0.8869
Da	PIN-4	0.8506	0.8113	0.8777	0.8510
goniometer	PIN-G	0.9254	0.8827	0.8897	0.8821
+Y (B, G), -Y (R, N)	HQE	1.0000	1.0338	0.9571	1.0793

Table 6: diode calibration correction factors
computed using Orbits 1314 (Cal-North) and 1912 (Cal-South), HQE blue as standard

Diode		Band			
position	type	BLUE	GREEN	RED	NIR
+Y	PIN-1	0.8927	0.8856	0.9178	0.8939
-Y	PIN-2	0.8990	0.8461	0.8994	0.8544
Df	PIN-3	0.8748	0.8571	0.9059	0.8825
Da	PIN-4	0.8402	0.8120	0.8784	0.8465
goniometer	PIN-G	0.9164	0.8849	0.8921	0.8777
+Y (B, G), -Y (R, N)	HQE	1.0000	1.0337	0.9573	1.0782

Table 7: diode calibration correction factors
computed using Orbits 1911 (Cal-North) and 1912 (Cal-South), HQE blue as standard

Diode		Band			
position	type	BLUE	GREEN	RED	NIR
+Y	PIN-1	0.8917	0.8769	0.9139	0.8922
-Y	PIN-2	0.8995	0.8406	0.8994	0.8553
Df	PIN-3	0.8810	0.8482	0.8946	0.8751
Da	PIN-4	0.8477	0.8040	0.8701	0.8427
goniometer	PIN-G	0.9230	0.8758	0.8810	0.8704
+Y (B, G), -Y (R, N)	HQE	1.0000	1.0300	0.9561	1.0682

Table 8: diode calibration correction factors
computed using Orbits 2575 (Cal-North) and 2585 (Cal-South), HQE blue as standard

Diode		Band			
position	type	BLUE	GREEN	RED	NIR
+Y	PIN-1	0.8912	0.8670	0.9101	0.8919
-Y	PIN-2	0.9000	0.8335	0.8961	0.8554
Df	PIN-3	0.8835	0.8472	0.9062	0.8905
Da	PIN-4	0.8436	0.7981	0.8738	0.8510
goniometer	PIN-G	0.9246	0.8722	0.8878	0.8839
+Y (B, G), -Y (R, N)	HQE	1.0000	1.0257	0.9536	1.0531

Table 9: diode calibration correction factors
computed using Orbits 3717 (Cal-North) and 3721 (Cal-South), HQE blue as standard

Diode		Band			
position	type	BLUE	GREEN	RED	NIR
+Y	PIN-1	0.8922	0.8590	0.9089	0.8936
-Y	PIN-2	0.8989	0.8248	0.8927	0.8561
Df	PIN-3	0.8717	0.8398	0.8967	0.8847
Da	PIN-4	0.8358	0.7969	0.8663	0.8510
goniometer	PIN-G	0.9147	0.8683	0.8785	0.8814
+Y (B, G), -Y (R, N)	HQE	1.0000	1.0212	0.9538	1.0330

The calibration correction factors are illustrated in a graphical manner in Figure 1 and Figure 2. The first figure shows that the PIN photodiodes have a systematic bias with respect to the HQE photodiodes. Perhaps the main difference between the two types of photodiodes aside from construction is that the HQE diodes use a trapped configuration whereas the PIN diodes are single detectors. The spectral filters all share a common heritage with those used in the MISR cameras. And, the diodes all share a common signal chain design. The hypothesis is that a systematic bias was introduced in the preflight calibration of the diodes, probably due to difficulties in characterizing the end-to-end spectral out-of-band response of the photodiodes.

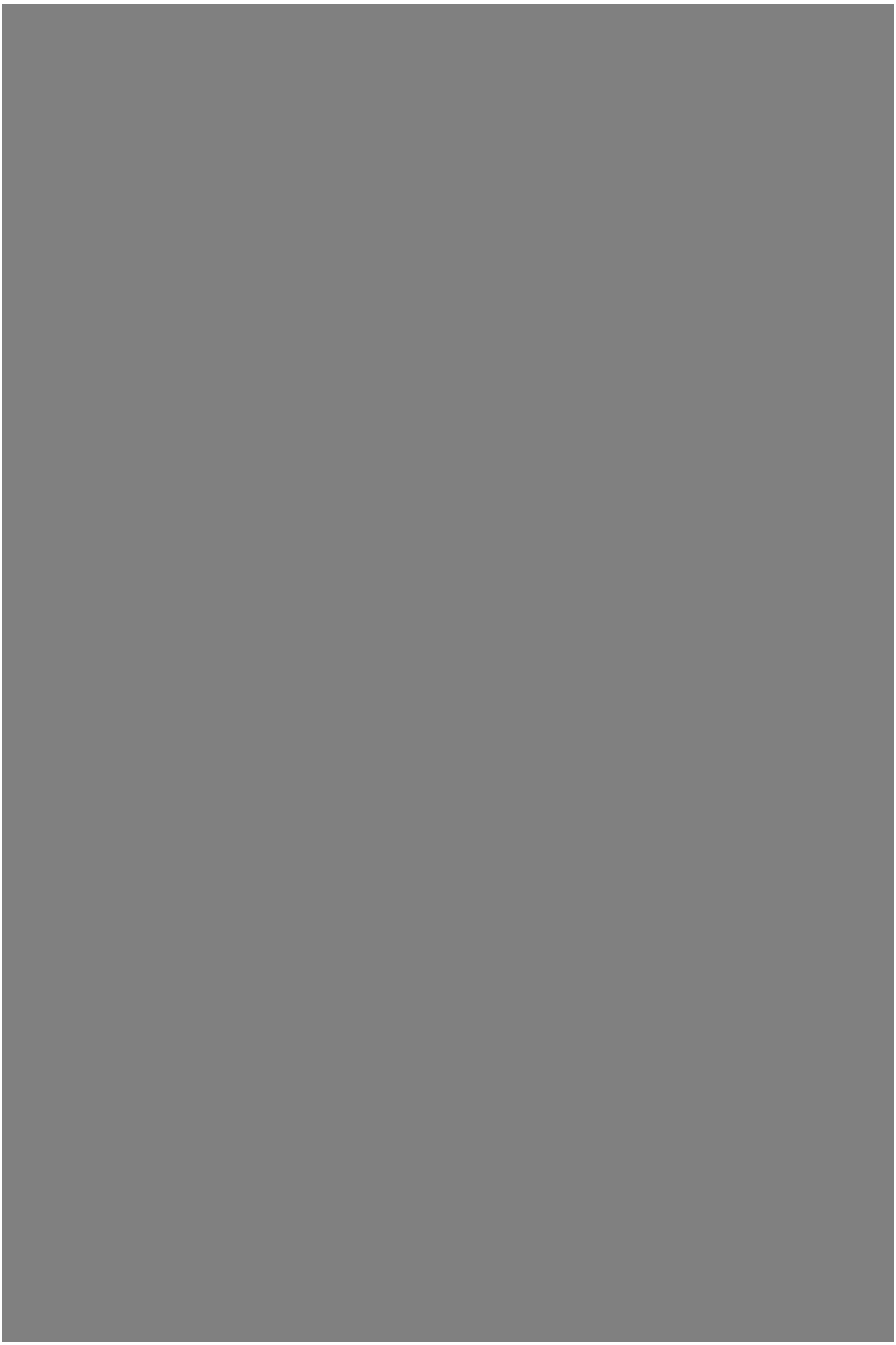

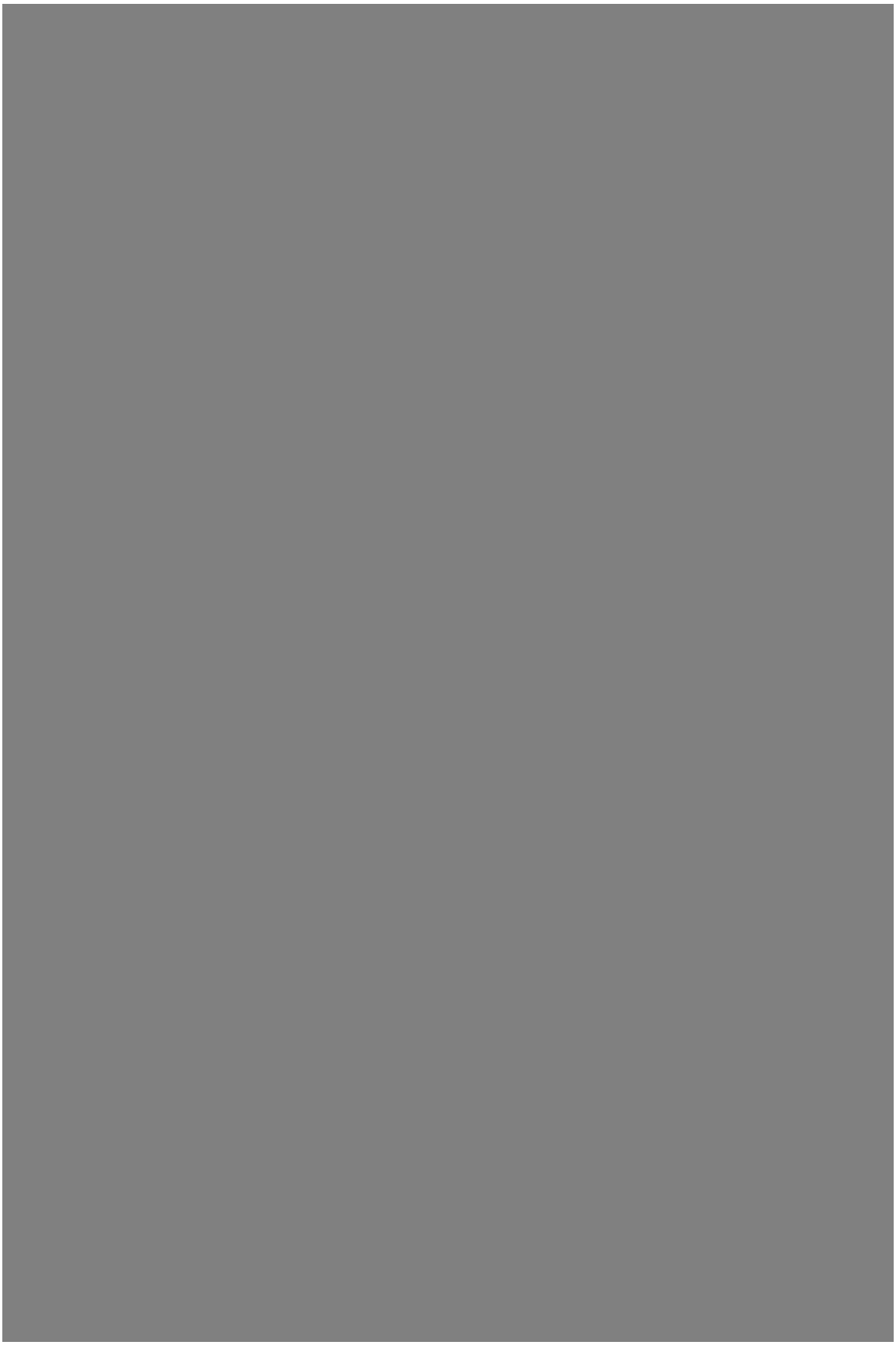

A simple means of evaluating the OBC performance was desired. The metric used is the average ratio of measured radiance to predicted radiance, $L_{\text{measured}}^{\text{std, OBC}} / L_{\text{predicted}}^{\text{std, OBC}}$, during the time that the goniometer is running. The time period that the goniometer is running was chosen as a straightforward way to ensure the average is taken when the panel is fully illuminated. Since the metric is a ratio, the closer to 1.0 the better. A radiance ratio that is greater than 1.0 indicates that the measured radiance is greater than the predicted value and a radiance ratio that is less than 1.0 indicates that the measured radiance is less than the predicted value.

The radiance ratio for each photodiode using the preflight diode calibrations is plotted as a function of time in Figure 3. Figure 4 and Figure 5 are plots of the radiance ratio when the Orbit 1259 calibration correction factors have been applied to the OBC results. Figure 4 is on the same scale as Figure 3, the preflight results, while Figure 4 is scaled to allow more detail to be seen. Both north and south data are presented on the same plot. The degradation in the green bands of the PIN diodes and the NIR HQE diode can be seen in the plots as well as in the larger standard deviations in the tables below of mean radiance ratio over all orbits. Table 12 is included to show that although the Cal-South data used to derive the "Orbit 1259 calibration correction factors" were from a different calibration sequence since the south panel was not being deployed at the time the Orbit 1259 data were acquired the results are still valid. It should be noted that the radiance ratios for the PIN-G diode are also averaged over the time period when the goniometer is running which means that the averages are also over all the viewing angles that the goniometer sampled.

In Figure 6, the radiance ratios that result when the OBC is calibrated for each calibration sequence are illustrated. This plot shows that data from Cal-South tends to measure slightly higher than the predicted radiance and to better match the predictions (ratio closer to 1.0) than the data from Cal-North. It is possible that the Cal-South panel better matches the measured Spectralon BRF data we acquired. It is also interesting to note that the D-diodes which actually view the calibration panels with the smallest zenith angles (nearest to a nadir-view) show the largest difference from the predicted radiance even after calibration correction factors are applied. The magnitude, however, is on a par with the results for the PIN-G (goniometer). Our ability to calibrate the PIN-G diodes is limited somewhat by the sparseness of nadir-viewing samples acquired during the time the goniometer is running.

Table 10: Ratio of measured radiance to predicted radiance using preflight diode calibrations

Pole	Diode	mean over all orbits				standard deviation over all orbits			
		BLUE	GREEN	RED	NIR	BLUE	GREEN	RED	NIR
Cal-North	PIN-1	0.875	0.870	0.902	0.879	0.003	0.019	0.008	0.006
	PIN-2	0.877	0.825	0.880	0.838	0.002	0.014	0.005	0.002
	PIN-4	0.807	0.794	0.859	0.832	0.005	0.016	0.012	0.005
	PIN-G	0.890	0.873	0.877	0.865	0.003	0.016	0.013	0.005
	HQE	0.973	1.021	0.945	1.051	0.003	0.010	0.005	0.025
Cal-South	PIN-1	0.896	0.878	0.914	0.897	0.001	0.018	0.004	0.002
	PIN-2	0.907	0.847	0.904	0.862	0.002	0.014	0.005	0.003
	PIN-3	0.902	0.893	0.941	0.929	0.005	0.019	0.008	0.006
	PIN-G	0.941	0.917	0.920	0.913	0.003	0.019	0.015	0.007
	HQE	1.013	1.026	0.952	1.067	0.001	0.008	0.002	0.023

Table 11: Ratio of measured radiance to predicted radiance using Orbits 1259/1912 diode calibrations

Pole	Diode	mean over all orbits				standard deviation over all orbits			
		BLUE	GREEN	RED	NIR	BLUE	GREEN	RED	NIR
Cal-North	PIN-1	0.980	0.980	0.983	0.984	0.004	0.022	0.009	0.006
	PIN-2	0.976	0.974	0.978	0.982	0.002	0.017	0.006	0.003
	PIN-4	0.949	0.978	0.979	0.977	0.006	0.019	0.014	0.006
	PIN-G	0.961	0.990	0.986	0.980	0.003	0.019	0.014	0.006
	HQE	0.973	0.987	0.988	0.974	0.003	0.009	0.005	0.024
Cal-South	PIN-1	1.003	0.990	0.996	1.003	0.001	0.020	0.005	0.003
	PIN-2	1.009	1.000	1.004	1.009	0.002	0.016	0.006	0.004
	PIN-3	1.022	1.045	1.042	1.047	0.006	0.022	0.009	0.007
	PIN-G	1.017	1.039	1.034	1.035	0.003	0.022	0.017	0.008
	HQE	1.013	0.992	0.995	0.989	0.001	0.008	0.002	0.021

Table 12: Ratio of measured radiance to predicted radiance using Orbits 1911/1912 diode calibrations[a]

Pole	Diode	mean over all orbits				standard deviation over all orbits			
		BLUE	GREEN	RED	NIR	BLUE	GREEN	RED	NIR
Cal-North	PIN-1	0.981	0.992	0.987	0.986	0.004	0.022	0.009	0.006
	PIN-2	0.975	0.981	0.979	0.980	0.002	0.017	0.006	0.003
	PIN-4	0.953	0.987	0.987	0.987	0.006	0.019	0.014	0.006
	PIN-G	0.964	0.997	0.996	0.994	0.003	0.019	0.014	0.006
	HQE	0.973	0.991	0.989	0.984	0.003	0.009	0.005	0.024
Cal-South	PIN-1	1.005	1.001	1.000	1.005	0.001	0.020	0.005	0.003
	PIN-2	1.009	1.008	1.005	1.008	0.002	0.016	0.006	0.004
	PIN-3	1.024	1.053	1.052	1.062	0.006	0.023	0.009	0.007
	PIN-G	1.020	1.047	1.044	1.049	0.003	0.022	0.017	0.008
	HQE	1.013	0.996	0.996	0.999	0.001	0.008	0.002	0.022

a. Differs from using Orbits 1259/1912 by at most 1.3%. Mean percent difference is 0.5%.

Table 13: Ratio of measured radiance to predicted radiance calibrating OBC for each calibration sequence

Pole	Diode	mean over all orbits				standard deviation over all orbits			
		BLUE	GREEN	RED	NIR	BLUE	GREEN	RED	NIR
Cal-North	PIN-1	0.980	0.984	0.984	0.982	0.003	0.004	0.004	0.004
	PIN-2	0.975	0.976	0.978	0.979	0.003	0.003	0.002	0.002
	PIN-4	0.954	0.976	0.975	0.976	0.003	0.005	0.005	0.005
	PIN-G	0.964	0.987	0.982	0.981	0.003	0.006	0.006	0.006
	HQE	0.972	0.988	0.987	0.980	0.003	0.003	0.003	0.004
Cal-South	PIN-1	1.005	1.001	1.001	1.003	0.001	0.001	0.002	0.001
	PIN-2	1.010	1.009	1.007	1.006	0.001	0.001	0.002	0.002
	PIN-3	1.023	1.046	1.042	1.049	0.005	0.004	0.007	0.007
	PIN-G	1.021	1.042	1.035	1.036	0.004	0.006	0.007	0.007
	HQE	1.013	0.997	0.997	1.005	0.001	0.001	0.001	0.001

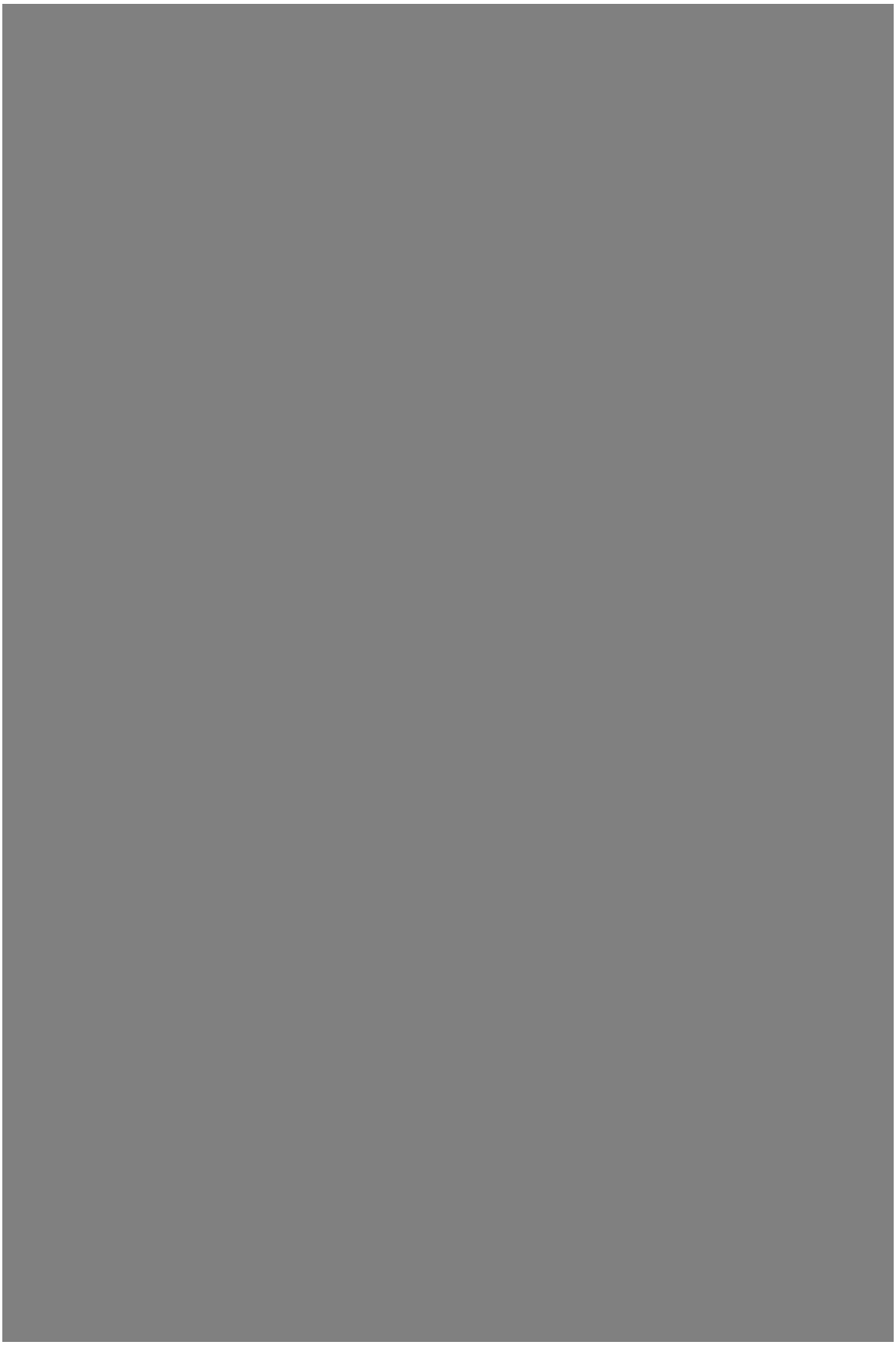

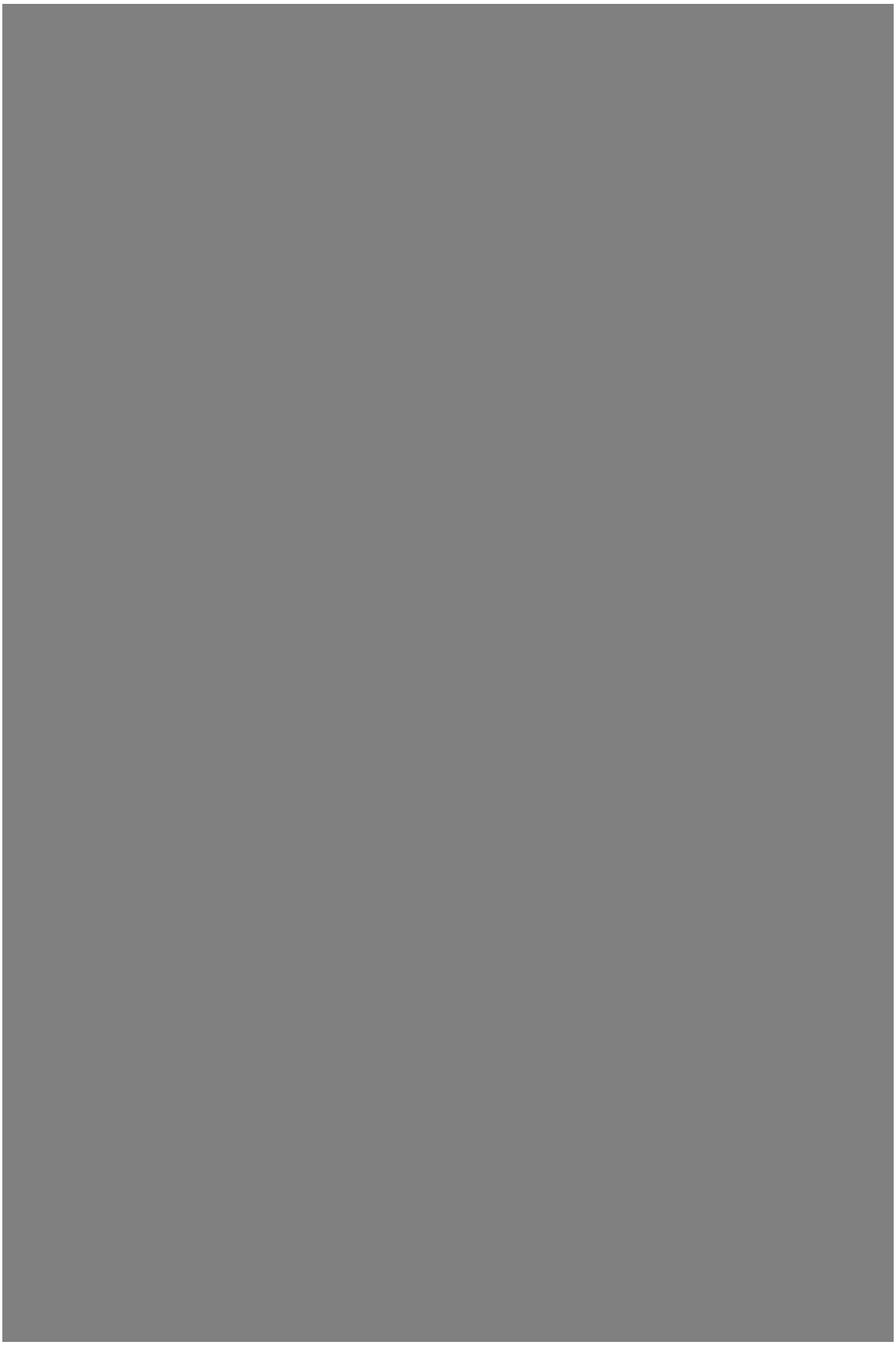

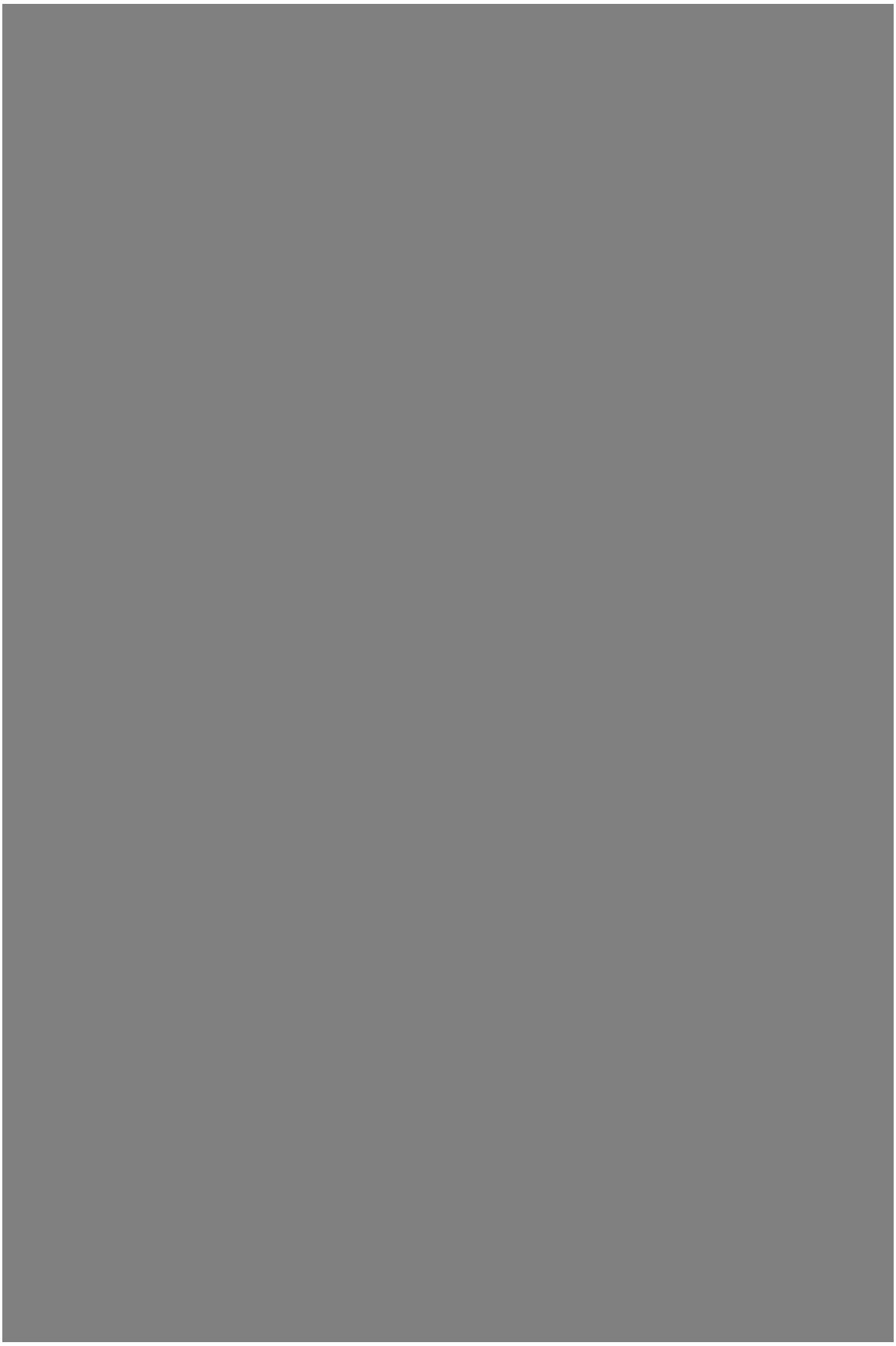

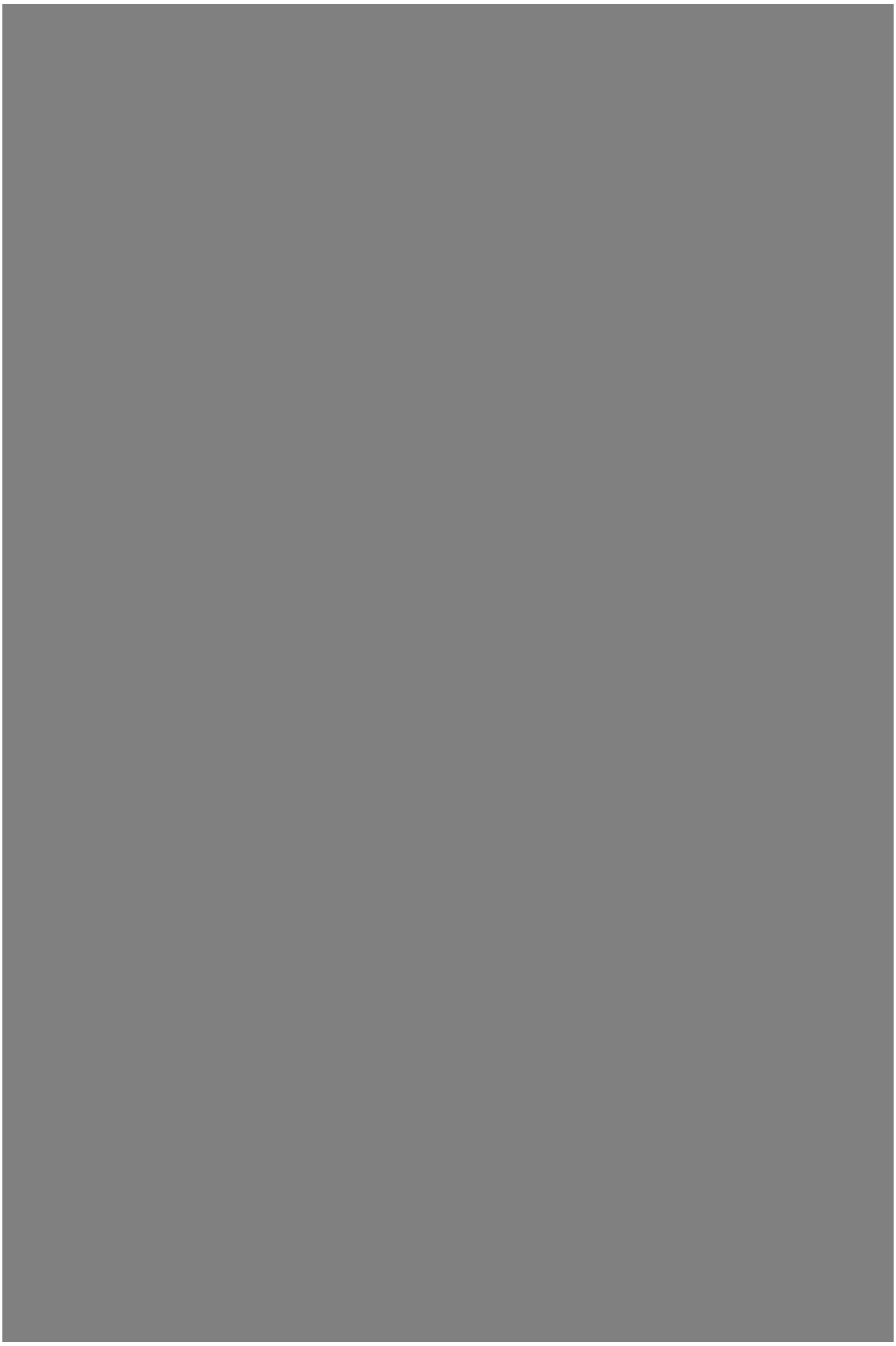

In conclusion, it is recommended that the OBC be re-calibrated to the HQE blue photodiode for each calibration sequence prior to the calibration of the MISR cameras, at least until such time as the HQE blue photodiode stability is called into question. The driving reason for this is the continued degradation shown in the HQE NIR photodiode.

Addendum

As a point of interest, the mean active pixel DN and mean overclock DN data contained in the ancillary data tables of the A-nadir CAL files were used along with the preflight, quadratic gain coefficients to compute the mean radiance measured by the A-nadir camera during the time that the goniometer was running during the various calibration sequences. A predicted radiance based on Equation 1 was also computed. However, rather than computing a radiance prediction for every pixel and then averaging, the BRF was interpolated for pixels 1, 376, 752, 1128, and 1504, the predicted radiance computed and an average taken. In Figure 7 note that for most of the Cal-North sequences the red and NIR bands are missing data due the averaging mode of the camera. Only 1x1 data was considered.

The plots show a degradation in the camera data of approximately 10% in all bands that is beginning to taper off, but does not appear to have completely stabilized as yet. The A-nadir camera also would appear to have started with a radiance that was almost 10% higher than the predicted radiance. This is the opposite of the preflight calibration of the PIN photodiodes.